Magnetism, Structure and the Effects of Thermal Aging on $(Fe_{1-x}Mn_x)_{73.5}Si_{13.5}B_9Nb_3Cu_1$ Alloys

Michelle R. Tamoria, E. E. Carpenter, M. M. Miller, J. H. Claassen, B. N. Das, R. M. Stroud, L. K. Kurihara, R. K. Everett, M. A. Willard, A. C. Hsiao, M. E. McHenry, and V. G. Harris

***Abstract*—Amorphous alloys of $(Fe_{1-x}Mn_x)_{73.5}$ $Si_{13.5}B_9$ Nb_3Cu_1, where $x = 0$, 0.05, 0.10, 0.15, were prepared by vacuum melt-spinning. Anneals performed at or above the crystallization temperature led to the formation of a nanostructure where the primary phase is a body centered cubic or DO_3 FeSi phase embedded within an intergranular amorphous phase. The saturation induction of the $x = 0.05$ alloy is 1.19 T, slightly lower than the parent alloy. Prolonged thermal aging led to an enhancement in the soft magnetic properties. This change occurs at soak times near 6000 s and corresponds to a decrease in the anisotropy and coercivity, and an increase in the remanent magnetization. EXAFS studies suggest that the Mn partitions during crystallization and thermal aging to the grain boundary regions may play an important role in enhancing the exchange coupling of the aged samples by increasing the Curie temperature of the amorphous intergranular phase.**

***Index Terms*—Composites, exchange coupling, nanostructures, permeability, soft ferromagnets.**

I. Introduction

In 1988, Yoshizawa, Oguma and Yamauchi [1] presented to the soft magnetic materials community a novel nanocomposite that consisted of FeSi grains embedded within an amorphous matrix. Since that time several alloys having similar morphologies, but differing chemistry, have been developed [2]. These alloys are attractive alternatives to Si–steels and metallic glasses since they possess moderate to high saturation induction, high permeabilities, and generally low core losses in the 10–100 kHz frequency range. These alloys often contain small amounts of Cu and Nb. Ayers *et al.* [3] have proposed that Cu catalyzes the nucleation of the primary grains and Nb partitions to the grain boundary where it stabilizes the glassy phase that suppresses grain growth.

In this paper, we explore the role of Mn substitution in the popular Finemet™ composition, $Fe_{73.5}Si_{13.5}B_9Nb_3Cu_1$. Previous studies of Cr substitution in this alloy have been reported by Franco *et al.* [4]. The addition of Cr results in a stabilization of the amorphous alloy increasing the crystallization temperature of the alloy. Increasing the Cr substitution results in a decrease in the Curie temperature (T_C) of the amorphous phase and a slightly smaller grain size [5].

We report here that thermal aging of Mn-substituted alloys led to a significant improvement in soft magnetic properties. We provide evidence that indicates the Mn resides in the amorphous phase after crystallization of the primary phase. The improvements in magnetic properties may correspond to the partitioning of Mn from the amorphous phase to the grain interface region thus increasing the T_C of the amorphous phase allowing for improved coupling between grains.

II. Experimental

$(Fe_{1-x}Mn_x)_{73.5}Si_{13.5}B_9Nb_3Cu_1$ alloys, where $x = 0.05$, 0.10, and 0.15, were arc-melted into ingots from elemental constituents having 99.99% purity, This was performed on a water-cooled Cu hearth under a positive pressure of Ar gas. The ingot was turned and remelted 3–4 times to ensure homogeneity throughout the ingot.

The arc-melted ingot was broken into 2–3 pieces and inserted into a quartz crucible having a small orifice at one end. The ingot was then inductively melted within its crucible under a partial pressure of He gas. The crucible was then pressurized using a positive pressure of He gas to expunge a molten stream onto a rotating Cu wheel (50 m/s) to form a quenched ribbon. The ribbons were heat treated to crystallization *in vacuo* at 490 °C, which was determined via differential scanning calorimetry (DSC) to be the onset of the primary crystallization.

The ribbons were characterized for their structural, physical and magnetic properties in both their as-spun and annealed states. Magnetic characterization was performed using vibrating sample and SQUID magnetometry, as well as a.c. permeability. The structural and physical properties were measured using X-ray diffraction, extended x-ray absorption fine structure (EXAFS), DSC, and microhardness.

III. Results and Discussion

$(Fe_{1-x}Mn_x)_{73.5}Si_{13.5}B_9Nb_3Cu_1$ alloys, where $x = 0.05$, 0.10, and 0.15, were melt-spun as free standing ribbons 2–3 mm in width, 20–30 micron thick, and several cms in length. Compared with the parent compound, increases in the Mn content brought about increased brittleness and reduced widths.

The increased brittleness precluded the formation of cores, hence the measurements described above were performed on ribbon sections having the same dimensions. This paper will deal largely with the structural and magnetic properties of the

Manuscript received October 13, 2000.

This work was supported by the Office of Naval Research.

M. R. Tamoria, E. E. Carpenter, M. M. Miller, J. H. Claassen, B. N. Das, R. M. Stroud, L. K. Kurihara, R. K. Everett, M. A. Willard, and V. G. Harris are with the Naval Research Laboratory, Washington DC 20375 USA (e-mail: harris@anvil.nrl.navy.mil).

A. C. Hsiao and M. E. McHenry are with the Materials Science and Engineering Department at Carnegie Mellon University, Pittsburgh, PA 15213 USA (e-mail: mm7g@andrew.cmu.edu).

Publisher Item Identifier S 0018-9464(01)06757-7.

Report Documentation Page

Form Approved
OMB No. 0704-0188

1. REPORT DATE	2. REPORT TYPE	3. DATES COVERED
OCT 2000		**00-00-2000 to 00-00-2000**

4. TITLE AND SUBTITLE	5a. CONTRACT NUMBER
Magnetism, Structure and the Effects of Thermal Aging on (Fe1 xMnx)73:5Si13:5B9Nb3Cu1 Alloys	5b. GRANT NUMBER
	5c. PROGRAM ELEMENT NUMBER
6. AUTHOR(S)	5d. PROJECT NUMBER
	5e. TASK NUMBER
	5f. WORK UNIT NUMBER
7. PERFORMING ORGANIZATION NAME(S) AND ADDRESS(ES) **Naval Research Laboratory,Washington,DC,20375**	8. PERFORMING ORGANIZATION REPORT NUMBER
9. SPONSORING/MONITORING AGENCY NAME(S) AND ADDRESS(ES)	10. SPONSOR/MONITOR'S ACRONYM(S)
	11. SPONSOR/MONITOR'S REPORT NUMBER(S)

12. DISTRIBUTION/AVAILABILITY STATEMENT
Approved for public release; distribution unlimited

13. SUPPLEMENTARY NOTES

14. ABSTRACT
see report

15. SUBJECT TERMS

16. SECURITY CLASSIFICATION OF:			17. LIMITATION OF ABSTRACT	18. NUMBER OF PAGES	19a. NAME OF RESPONSIBLE PERSON
a. REPORT **unclassified**	b. ABSTRACT **unclassified**	c. THIS PAGE **unclassified**	**Same as Report (SAR)**	**4**	

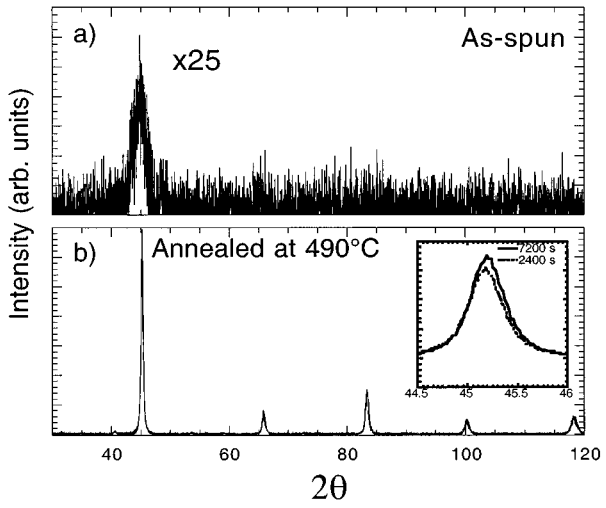

Fig. 1. $\theta - 2\theta$ x-ray diffraction patterns for the $(Fe_{1-x}Mn_x)_{73.5}Si_{13.5}B_9Nb_3Cu_1$ alloy where $x = 0.05$. Data sets that correspond with the (a) as-spun ribbon and (b) ribbons annealed at 490 °C for 2400 s and 7200 s are presented. Inset of (b) is an expanded view of the (110) peak illustrating slight changes due to thermal aging. Lattice parameter analysis is presented in the text.

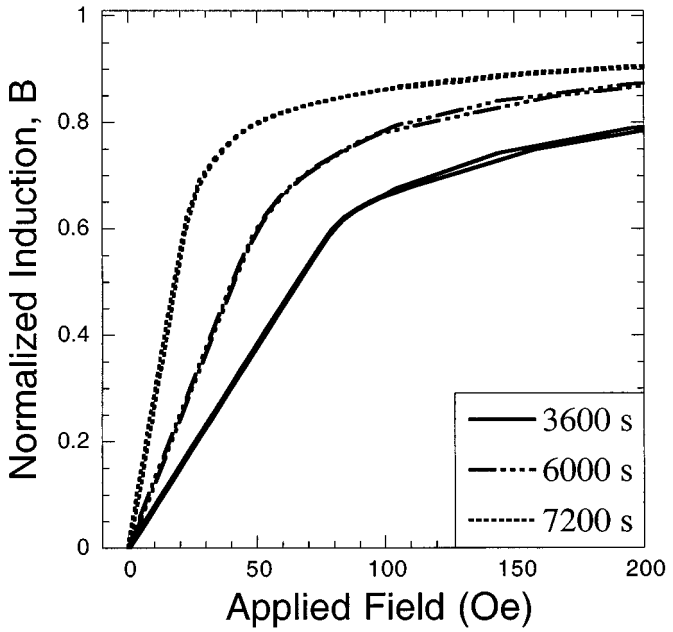

Fig. 2. First quadrants of the BH loops collected from three samples of the Mn = 0.05 substituted alloy having soak times ranging from 3600–7200 s at 490 °C. Saturation induction has been normalized to values at H = 10 kOe.

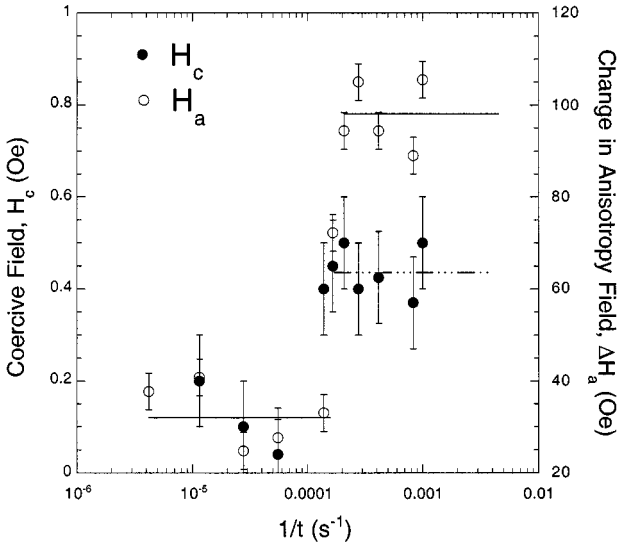

Fig. 3. Coercive and anisotropy fields versus soak time as $1/t$ (s^{-1}). A change in anisotropy field is measured with a baseline value determined by shape anisotropy.

Mn = 0.05 substituted alloy and the effects of thermal aging on this alloy.

Relative hardness, measured using a Buehler Micromet II Digital Vickers Microhardness Tester, increased linearly with thermal aging. This trend is observed in all alloys with the slope of change greater in the Mn-containing alloys, but the absolute values higher in the parent alloy. It is noteworthy that the hardness does not plateau for the aging times studied here suggesting that continued aging improves the relative hardness of these nanocomposites.

X-ray diffraction $\theta - 2\theta$ scans were performed on all alloys before and after heat treatment. Fig. 1 is a plot of XRD pattern for the as-spun Mn = 0.05 alloy [see Fig. 1(a)] and the same after 2400 s and 7200 s at 490 °C [see Fig. 1(b)]. The pattern corresponding with the as-spun alloy is consistent with an amorphous alloy. Specifically, there is a diffuse peak near 44° in 2θ with no other features detectable above the background.

Note that the as-spun alloy amplitude is multiplied by 25 in order to allow comparisons to the crystalline equivalent. The region of the crystallized data encompassing the (110) peak is presented in an expanded view as the inset plot to Fig. 1(b). The crystallized samples show 5 diffraction peaks over the scan range. All of these features can be readily indexed to a bcc phase. From our knowledge of the parent compound, it is possible that this phase is a DO_3 FeSi phase [3]. Scherrer analysis indicates that the particle size is 7 nm for the sample annealed for 120 min and 4 nm for the sampled annealed for 40 min [6].

The lattice parameter calculated for the sampled annealed for 2400 s and 7200 s are 2.8387 ± 0.0006 Å and 2.8374± 0.0008 Å, respectively. Similar values for the parent compound are 2.8381 ±1 0.00 Å (3600 s at 550 °C) and 2.8383 ± 0.0002 Å (7200 s at 550 °C). This agreement in lattice parameter for alloy Mn = 0 and Mn = 0.05 suggests that the Mn does not substitute in the FeSi lattice.

The crystallization kinetics of this alloy is the subject of a separate paper by Hsaio *et al.* [6].

Fig. 2 is a plot of the first quadrant of the Mn = 0.05-substitute alloy's BH loops for three samples annealed at 490 °C for soak times of 3600 s, 6000 s and 7200 s. The induction of each has been normalized and plotted on the same axes to illustrate the change in d.c. permeability as a function of thermal aging. These plots have been carefully chosen to show the most dramatic changes occur during soak times around 6000 s.

Fig. 3 is a plot of the anisotropy fields collected from the extrapolation of the linear region of the $M - H$ loops for the Mn = 0.05 substituted alloy. A dramatic drop in anisotropy field (corresponding to an increase in permeability) is measured to occur at $1/t = 0.0002$ s^{-1}. Correspondingly, the coercive field

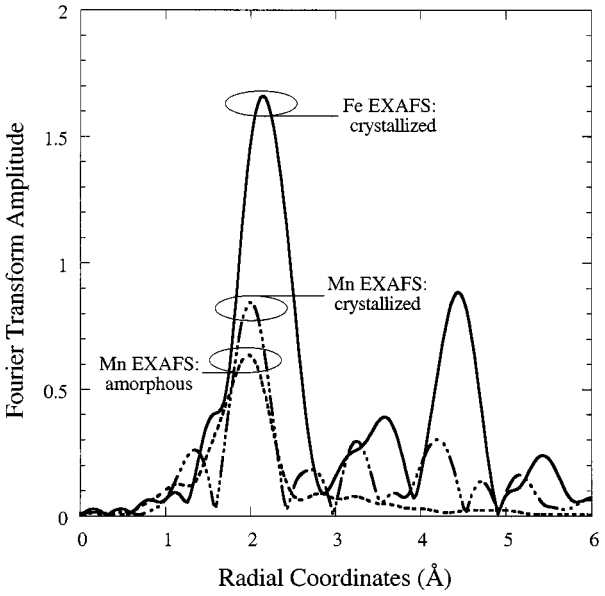

Fig. 4. Fourier transformed Mn and Fe EXAFS collected from the Mn = 0.05 substituted alloy and its parent alloy before and after crystallization.

(see Fig. 3) is also reduced substantially, while the remanent magnetization increases over the same range of times suggesting an increase in the exchange coupling. The saturation induction (B_S) is measured to decrease slightly with soak time from the effects of oxidation.

The a.c. permeability is measured to increase 25–30% in the crystallized samples as compared with the as-spun amorphous alloys. The measurement method follows that described by Kumasaka *et al.* [7]. Values for the Mn = 0.05 substituted alloy ($\mu_{10\,\mathrm{kHz}} = 450$) after crystallization and thermal aging are comparable to those of the parent alloy and in some cases exceed them.

EXAFS studies were performed on Mn atoms in the Mn-substituted and the parent alloys before and after anneals (see Fig. 4). Fig. 4 are Fourier transformed Mn and Fe EXAFS data. The Fourier transform of EXAFS data is an element specific radial distribution function where the peaks correspond to atomic shells and their centroids correspond to bond distances [8].

The local environment of the Mn atoms in the as-spun ribbons (dashed curve in Fig. 4) are consistent with an amorphous environment. In this Fourier profile the near neighbor peak is well defined and no other peaks appear above the background. After anneals, the Mn EXAFS show the appearance of higher order peaks that confirm crystallization. However, the atomic symmetry does not appear to be bcc and has not yet been identified. In comparison, Fourier transformed Fe data are plotted as a solid curve. These data have been identified as being similar to the bcc symmetry [3]. Clear differences are observed between the crystallized Mn and crystallized Fe data.

The amplitude of the crystallized Mn data is a factor of 2 smaller than that of Fe, but only ∼20% larger than the disordered amorphous Mn signal. The reduced amplitude of the amorphous signal stems from the effects of very large static disorder intrinsic to the glass-like environment of transition metal atoms in amorphous systems.

The average Mn environment in the annealed samples is also highly disordered. This would not be expected if Mn atoms were to substitute for Fe atoms in the bcc phase. From these results we conclude that Mn remains in a highly disordered phase after the primary crystallization of FeSi.

We propose that upon thermal aging the Mn atoms migrate from the amorphous region to the interface region separating the FeSi grains from the amorphous matrix. The decrease of Mn in the amorphous region increases the T_C of the amorphous phase thus enhancing the exchange between grains. A fingerprint of the improved exchange coupling is seen in the increased remanent magnetization also coinciding with the reduced anisotropy field and coercivity.

IV. Summary

1) Mn-substituted alloys of the Finemet™) composition were processed via vacuum melt spinning. The ribbons are 2–3 mm in width, several cm in length and 20–30 microns thick. The substituted alloys are more brittle than their parent alloy and brittleness is measured to increase with Mn content. The ribbons were too brittle to process as cores.
2) Mn substitution of the parent alloy leads to a reduction in the crystallization temperature. However, the lattice parameter of the crystalline phase is nearly identical to the FeSi crystals of Finemet™) and does not change within the measurement's uncertainty with thermal aging.
3) Thermal aging above the crystallization temperature for times in excess of 6000 s leads to a reduction in anisotropy and coercivity. Remanent magnetization is measured to increase under the same conditions.
4) Relative microhardness is measured to increase linearly with thermal aging. This trend is observed in all alloys with the slope of change greater in the Mn-containing alloys with the maximum value being higher in the parent alloy.
5) a.c. permeability is measured at 10 kHz to increase with the crystallization of the alloy. The values for the Mn-substituted alloys are comparable to the parent alloy and in some cases are greater.
6) EXAFS measurements of the Mn and Fe in the parent and substituted alloys, before and after crystallization, reveal that the Mn environment after annealing remains highly disordered suggesting that the Mn resides in the grain boundary region after the anneals.
7) We propose that the thermal aging of the sample induces the migration of Mn atoms to the interface between the grains and the amorphous regions, increasing the T_C of the amorphous phase, and improving the coupling between grains.

References

[1] Y. Yoshizawa, S. Oguma, and K. Yamauchi, "New Fe-based soft magnetic alloys composed of ultrrafine grain structure," *J. Appl. Phys.*, vol. 64, pp. 6044–6046, 1988.
[2] M. E. McHenry, M. A. Willard, and D. E. Laughlin, "Amorphous and nanocrystalline materials for applications as soft magnets," *Prog. Mat. Sci.*, vol. 44, pp. 291–434, 1999.

[3] J. D. Ayers, V. G. Harris, J. A. Sprague, W. T. Elam, and H. N. Jones, "On the formation of nanocrystals in the soft magnetic alloy $Fe_{73.5}Si_{13.5}B_9Nb_3Cu_1$," *Acta Mater.*, vol. 46, no. 6, pp. 1861–1874, 1998.

[4] V. Franco, C. F. Conde, and A. Conde, "Changes in magnetic anisotropy distribution during structural evolution of $Fe_{76}Si_{10.5}B_{9.5}Nb_3Cu_1$," *J. Magn. Magn. Mater.*, vol. 185, pp. 353–359, 1998.

[5] V. Franco, C. F. Conde, A. Conde, B. Varga, and A. Lovas, "Thermomagnetic study of $Fe_{73.5-x}Cr_xSi_{13.5}B_9Nb_3Cu_1$ ($x = 1$, 3, 5, 10) alloys," *J. Magn. Magn. Mater.*, vol. 215–216, pp. 404–406, 2000.

[6] A. C. Hsiao, M. E. McHenry, D. E. Laughlin, M. R. Tamoria, and V. G. Harris, "Magnetic properties and crystallization kinetics of a Mn-doped Finemet™ precursor amorphous alloy," *IEEE Trans. Magn.*, vol. 37, no. 4, July 2001.

[7] N. Kumasaka *et al.*, "Magnetic properties of multilayered FeSi films," *J. Appl. Phys.*, vol. 55, no. 6, pp. 2238–2249, 1984.

[8] "Electron phase shift corrections have not been included at this stage in the analysis. The peak positions of the Fourier transformed EXAFS data do not correlate directly with bond distances but are instead shifted by an amount equal to the electron phase shift of the pair correlations contributing to the Fourier peaks,".

[9] V. Franco, C. F. Conde, and A. Conde, "Magnetic properties and nanocrystallization of a $Fe_{63.5}Cr_{10}Si_{13.5}B_9Nb_3Cu_1$ alloy," *J. Magn. Magn. Mater.*, vol. 203, pp. 60–62, 1999.